

# Chapter 7

## Flow Cytometric and Laser Scanning Microscopic Approaches in Epigenetics Research

Lorant Szekvolgyi, Laszlo Imre, Doan Xuan Quang Minh, Eva Hegedus, Zsolt Bacso, and Gabor Szabo

### Abstract

Our understanding of epigenetics has been transformed in recent years by the advance of technological possibilities based primarily on a powerful tool, chromatin immunoprecipitation (ChIP). However, in many cases, the detection of epigenetic changes requires methods providing a high-throughput (HTP) platform. Cytometry has opened a novel approach for the quantitative measurement of molecules, including PCR products, anchored to appropriately addressed microbeads (Pataki et al. 2005. *Cytometry* **68**, 45–52). Here we show selected examples for the utility of two different cytometry-based platforms of epigenetic analysis: ChIP-on-beads, a flow-cytometric test of local histone modifications (Balint et al. 2005. *Mol. Cell Biol.* **25**, 5648–5663), and the laser scanning cytometry-based measurement of global epigenetic modifications that might help predict clinical behavior in different pathological conditions. We anticipate that such alternative tools may shortly become indispensable in clinical practice, translating the systematic screening of epigenetic tags from basic research into routine diagnostics of HTP demand.

**Key words:** Chromatin immunoprecipitation (ChIP), flow cytometry, ChIP-on-beads, laser scanning cytometry (LSC).

### 1. Introduction

Epigenetic changes associated with gene regulation play a major role in the establishment of altered differentiation states (3). Specific modifications often correlate with gene activation or repression; for instance H3K4ac and H3K4me3 are permissive for gene activation whereas H3K9me2, H3K27me3, and methylation of CpG islands in promoter regions correlate with transcriptional silencing. Often, activating and repressive marks co-exist at gene start sites, reflecting perhaps epigenetic heterogeneity among otherwise similar cells, establishing a fine balance that could determine the gene expression patterns in the tissue.

The ‘epigenetic code’ has become an indispensable concept in basic research, and its principles are also utilized to develop drugs and diagnostic tools. Several genes being epigenetically misregulated have been shown to associate with different kinds of cancer, highlighting the role of the ‘language’ of covalent modifications in tumorigenesis (4, 5). For instance, based on the patterns of modifications, two disease subtypes with different risks of tumor recurrence have been characterized in prostate cancer patients, independently from tumor stage, preoperative prostate-specific antigen levels, and capsule invasion (6).

The chromatin of cancer cells often exhibits both an overall (global) DNA hypomethylation and hypermethylation of specific regions, leading to ‘DNA methylation imbalance’ (7). The recurrence of global DNA hypomethylation in many types of human cancer is suggestive of its significant role in carcinogenesis, perhaps by inducing genomic instability and/or activating oncogenes (8, 9). However, global hypomethylation is subject to a high degree of variability, unaccounted for by our current level of understanding (10, 11). In addition to neoplastic transformation, problems of epigenetic regulation, including CpG methylation disorders are also involved in a wide range of pathological phenomena (12, 13). In most eukaryotes, methylation of DNA occurs at the cytosine residues of cytosine-phospho-guanine (CpG) dinucleotides. The enzymes responsible for the production of 5-methylcytosine (5-mc) involving the fifth carbon atom of cytosine in CpG dinucleotides are the DNA methyltransferases DNMT1, DNMT3a, and DNMT3b, of which the first is involved in the maintenance of methylation during DNA replication, while all appear to be important in the establishment of methylation patterns in most physiological and pathological settings (14–16).

### 1.1. Flow- and Laser Scanning Cytometry in Epigenetics Research

Our understanding of epigenetics has been transformed in recent years by a succession of technological innovations. Approaches involving microarrays and, most recently ultra-high throughput (deep) sequencing technology have been applied to map cytosine methylation, chromatin modifications, and ncRNAs across entire genomes. Genome-scale studies of histone modifications and other aspects of chromatin structure typically rely on an immunological procedure, chromatin immunoprecipitation (ChIP) (17), in which specific antibodies are used to enrich chromatin. ChIP is a powerful tool in epigenetics; however, in many cases the detection of epigenetic changes or transcription factor binding associated with the regulation of certain genes would require ChIP-based methods that provide high-throughput (HTP) potential. Monitoring local as well as global changes of epigenetic markers could be extremely useful in diagnostics as well as in basic research.

Flow-cytometric analysis provides a novel means for the quantitative measurement of molecules also in cell-free solutions, anchoring them to appropriately addressed microbeads. The utility and power

AQ1

## Flow Cytometric and Laser Scanning Microscopic Approaches

of this approach has been demonstrated in the case of various assays of molecular diagnostic value: immunoassays, sensitive measurement of protease or nuclease activity, detection of deletion/insertion of sequences by heteroduplex analysis, etc., that could all be adapted to a 'lab-on-beads' platform, i.e., the flow-cytometric analysis of microbead-captured macromolecules (1, 18, 19). Many samples can be simultaneously analyzed in a FACSarray instrument using fluorescent dyes matching its optical channels.

Beyond lending a HTP platform for the analysis of gene-specific epigenetic markers, cytometry also makes global analysis of epigenetic changes possible, most conveniently in its on-slide format, by microscope-based cytometers. Laser scanning cytometry (LSC) provides a robust method for analyzing single-cell events on slides (20, 21). It generates quantitative fluorescence data similar to flow cytometry, but the analyzed cells are attached to the surfaces of microscopic slides or culture chambers. The main advantages of LSC are that (i) the possible correlation between the simultaneously measured parameters is detected at the individual cell resolution, i.e., with a sensitivity surpassing that of flow cytometry; (ii) the instrument is able to relocate each cell for additional measurements, thus the analysis of functional features of live cells can be combined with measurements that require fixed cells; and (iii) measurements can be performed in an automated fashion, pre-programmed for several slides.

Examples highlighted in this review demonstrate the value of two different HTP platforms for epigenetic analysis, namely ChIP-on-beads and assessment of global epigenetic traits by LSC. These methods might help introduce systematic screening of different epigenetic tags into clinical practice, especially of those that correlate with therapeutic success. It will be shown that sequence-specific capture of PCR-amplified ChIP-fragments on microbeads allows a robust detection of histone-tail modifications in the promoter region of a well-characterized gene, tissue transglutaminase type 2 (*TGM2*). We also assess the prospects of laser scanning cytometry for the analysis of epigenetic changes involving the whole genome via the example of a global DNA methylation test.

134  
135 **1.2. High-Throughput**  
136 **Screening of Local**  
137 **Epigenetic Changes**  
138 **by ChIP-on-Beads**

We have investigated the cellular levels of H4K acetylation and H3K4 methylation of the histone tails at the promoter of the *TGM2* gene, to test whether these covalent modifications can be detected using a flow-cytometric platform. As shown earlier (2) and briefly recapped herein, the flow-ChIP method, nicknamed ChIP-on-beads, can be easily implemented in a routine flow-cytometric clinical laboratory without relying on real-time QPCR. In the ChIP-on-beads assay, a standard ChIP is performed and then this DNA is used as template in an end-point PCR reaction. The sense and anti-sense primers are tagged at their 5' ends with fluorescent dyes (e.g., Fam, Cy3) and biotin,

145  
146  
147  
148  
149  
150  
151  
152  
153  
154  
155  
156  
157  
158  
159  
160  
161  
162  
163  
164  
165  
166  
167  
168  
169  
170  
171  
172  
173  
174  
175  
176  
177  
178  
179  
180  
181  
182  
183  
184  
185  
186  
187  
188  
189  
190  
191  
192

respectively. Small aliquots of the Fam/biotin-ended PCR products are then bound to streptavidin-conjugated microbeads and quantified by flow cytometry. Of note, PCRs must be stopped in the linear phase to ensure reliable quantification; this should be initially determined in pilot QPCR experiments. The similarity of data obtained by QPCR and by flow cytometry has been shown (2).

As shown in Fig. 7.1A, the fluorescence intensity of the microbeads increases linearly with the quantity of the fluoresceinated PCR products added, allowing the expression of ChIP-PCR

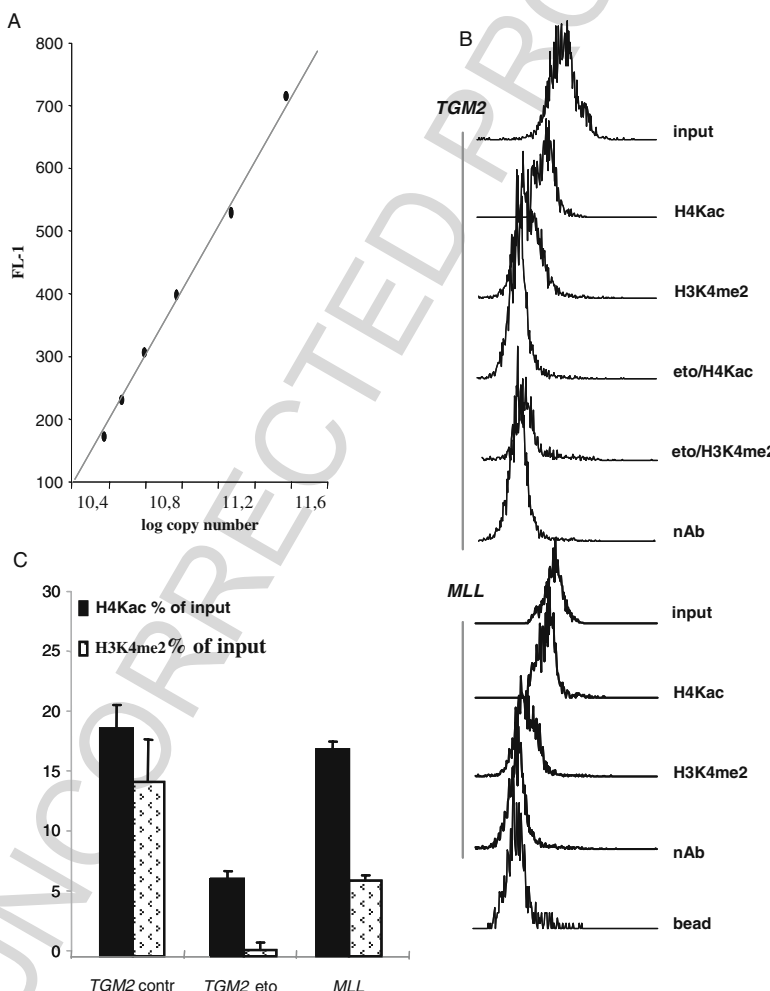


Fig. 7.1. Analysis of gene specific histone modifications by ChIP-on-beads. (A) Calibration curve (FL-1 vs. log copy number) based on a dilution series of known quantities of Fam/biotin-tagged PCR products. *TGM2* copy numbers of ChIP-PCR samples were determined by reference to this standard curve. (B,C) ChIP-on-beads analysis of H4Kac and H3K4me2 histone modifications at the *TGM2* gene promoter and at exon 9 of the *MLL* gene, in Jurkat cells. Apoptosis was induced by etoposide treatment (Eto). (B) Flow-cytometric fluorescence distribution histograms of Fam/biotin-labeled ChIP-PCR samples captured on streptavidin-conjugated microbeads. (C) The level of modified histones within the *TGM2* and *MLL* genes are expressed as percent of input values (Y axis), based on the means of fluorescence distribution and after subtracting the background (i.e., no-antibody % of input values). Panels (B) and (C) were reproduced from (2).

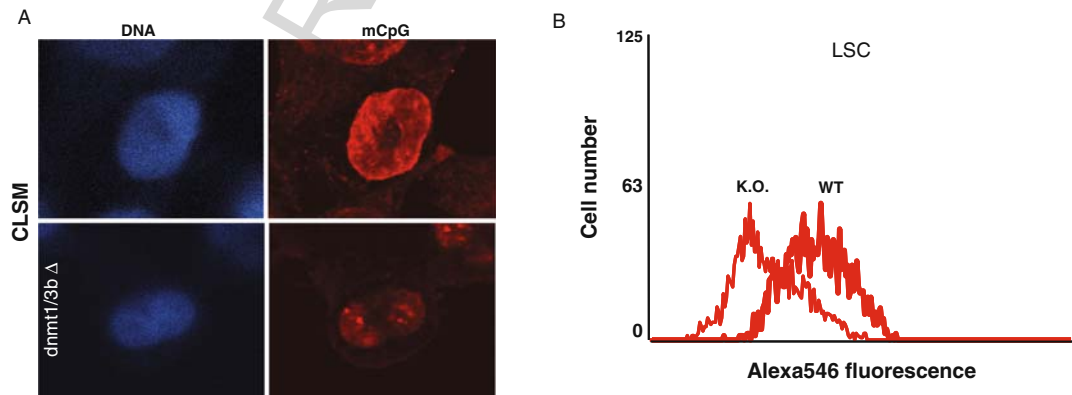
## Flow Cytometric and Laser Scanning Microscopic Approaches

193 yields as absolute copy numbers. The flow-cytometric fluorescence  
 194 distribution means are used to calculate the fraction of DNA copy  
 195 numbers in the ChIP samples relative to the input DNA  
 196 (**Fig.7.1B**). Comparing control and early-apoptotic Jurkat cells  
 197 for changes in the level of H4Kac and H3K4me within the pro-  
 198 moter of *TGM2*, we observed a significant decrease in both histone  
 199 modifications (**Fig.7.1C**), suggestive of the closure of chromatin  
 200 structure early upon apoptosis. In comparison, the observed his-  
 201 tone modifications at exon 9 of the *MLL* gene, used as positive  
 202 control, were in accordance with its known histone-code profile  
 203 (22); in contrast, the  $\beta$ -globin gene, used as negative control, gave  
 204 <0.1% Ab/input ratios (not shown).

205  
 206 **1.3. Testing Global**  
 207 **Epigenetic Changes**  
 208 **by Laser Scanning**  
 209 **Microscopy: Studies**  
 210 **on DNA Methylation**

211 It is often important to consider in what global context local  
 212 epigenetic changes occur (23). Moreover, global changes of cer-  
 213 tain epigenetic modifications may have their independent diagno-  
 214 stic value, especially when analyzed in correlation with other  
 215 phenotypic markers, an opportunity offered by up-to-date laser  
 216 scanning microscopic systems (20, 21). Development of antibo-  
 217 dies and chimeric methyl CpG-binding antibody-like proteins  
 218 (24–27), both recognizing CpG with high specificity, has opened  
 219 novel perspectives for the diagnostic analysis of global methylation  
 220 states. Anti-5mC antibodies are commercially available through  
 221 various sources (e.g., Abcam and Biocarta US).

222 In experiments using the recombinant mCpG-binding anti-  
 223 body-like MBD-Fc protein (26–28), the overall level of CpG  
 224 methylation has been quantified in the HCT116 cell line  
 225 (**Fig.7.2**). As shown by confocal laser scanning microscopy



226 Fig. 7.2. Global DNA methylation analyzed by confocal laser scanning microscopy and laser scanning cytometry. *WT*: wild-  
 227 type *DNMT1/DNMT3b* HCT116 cells immunolabeled with the MBD-Fc fusion protein. *K.O.*: *dnmt1/dnmt3b* knock-out  
 228 HCT116 cells immunolabeled with the MBD-Fc fusion protein. *Left slides*: DNA stained by Hoechst. *Right slides*:  
 229 methylated DNA (mCpGs). (**A**) Methylated CpG dinucleotides visualized by confocal laser scanning microscopy (CLSM).  
 230 (**B**) Sample analyzed by laser scanning cytometry (LSC). MCpG (red) fluorescence was quantified in the slide-attached  
 231 cells ( $n>400$ ) and presented (in arbitrary units) as fluorescence distribution histograms.

This figure will be printed in b/w

(CLSM), mCpGs have been efficiently labeled by indirect immunofluorescence in *DNMT1/3b* wild-type and, to a lesser extent, *DNMT1/3b* double knock-out cells. The level of mCpGs has been quantified in a sizable population of cells by an iCys laser scanning cytometer and iCyte 2.6 software (CompuCyte, USA). As shown in Fig.7.2, the fluorescence distributions of the Alexa546-labeled mCpGs are significantly different in the *DNMT1/3b<sup>+/−</sup>* cells; this result demonstrates the utility of LSC for the fine assessment of global methylation states in different cell types (e.g., differentiated vs. stem cells) or in a specific cell type (e.g., in human peripheral lymphocytes isolated from blood samples) before and after drug treatment or chemotherapy. Since LSC can be performed in an automated fashion, such studies could be made on large sets of biopsy material so as to establish the exact role of global DNA methylation in human pathological diagnosis of various diseases.

Data presented herein have demonstrated that if combined, flow cytometry and conventional PCR offer a powerful tool in the quantitative analysis of ChIP results. We have found high levels of H4Kac and H3K4me at the *TGM2* gene core promoter (Fig.7.1). These levels significantly decreased upon apoptosis and this was accompanied by the down-regulation of *TGM2* mRNA expression (2), suggesting that this enzyme does not contribute to the early manifestations of apoptosis in Jurkat cells. Differences in the global level of DNA methylation in HCT116 wild-type and methylation defective cells have been revealed by LSC, the on-slide version of flow cytometry (Fig.7.2). Both assays can be easily implemented, and readily applied in a HTP format. We envisage the utility of these platforms primarily in clinical screening efforts addressing one, or a few, epigenetic markers in many samples simultaneously, depending on cost/time considerations and availability of instrumentation/expertise.

Although the epigenetic changes are heritable, they appear to be readily reversed by specific drug treatments as opposed to gene mutations. We expect that the epigenetic silencing of, e.g., tumor suppressor genes will soon become a frequent target of HTP screening studies because these mechanisms may be as important in carcinogenesis as the inactivating mutations. Drugs targeting the enzymes that remove or add these chemical tags are at the forefront of research: diseases to be targeted include cancer, imprinting disorders, autoimmune diseases, certain neurological disorders, diabetes, cardiopulmonary diseases, in which mis-steps in epigenetic programming have been directly implicated. Pharmaceutical companies have set up programs on histone deacetylases (HDACs) and DNA methyltransferases (DNMTs) and their inhibitors, as they have the potential to re-activate specific tumor suppressor genes; clinical trials being on the way are promising the prospect of eliciting tumor regression by modulation of epigenetic regulation.

## Flow Cytometric and Laser Scanning Microscopic Approaches

289 Based on the above, we anticipate that epigenetic analysis will  
290 enter routine diagnostic practice whenever monitoring epigenetic  
291 markers can help predict clinical behavior. When large sets of  
292 samples are to be assessed, high-throughput platforms for the  
293 accurate evaluation of the ChIP results are of general interest. In  
294 view of the fact that most routine techniques can be adapted to  
295 flow cytometry which exceeds more conventional methods in  
296 sensitivity and reproducibility, the approaches shown can provide  
297 a universal platform for almost any kind of lab purposes. Whether  
298 ChIP-QPCR, ChIP-on-beads, or LSC-based assays of global epi-  
299 genetic changes will be selected as the approach of choice for such  
300 screening projects will be determined by the particular task under-  
301 taken, and the capabilities of the clinical laboratories. We believe  
302 that these alternative ChIP platforms can help bring epigenetic  
303 analysis within reach for routine laboratories, especially for those  
304 involved in clinical diagnostics.

---

**2. Materials****2.1. Cell Culture**

- 311 1. McCoy's medium (Sigma-Aldrich).
- 312 2. Solution of trypsin: stock solution at 0.5%, working solution  
313 at 0.05% in 1X phosphate buffered saline (PBS); store at –  
314 20°C.
- 315 3. Glutamine: stock solution at 200 mM, final concentration at 2  
316 mM in ddH<sub>2</sub>O; store at –20°C.
- 317 4. Etoposide (Sigma-Aldrich): stock solution at 40 mM, work-  
318 ing concentration at 40 µM.

**2.2. Detection  
of Methylated CpGs by  
Immunofluorescence**

- 321 1. 1X PBS: 1.37 MNaCl, 27 mM**K**Cl, 100 mM**Na**<sub>2</sub>HPO<sub>4</sub>, 18  
322 mM**KH**<sub>2</sub>PO<sub>4</sub>; adjust to pH 7.4 with HCl if necessary.
- 323 2. Labeling solution: 1X PBS/10%BSA; store at –20°C.
- 324 3. Primary antibody (1.9 mg/mL): MBD-Fc, a recombinant  
325 antibody which was made of human MBD domain (methyl  
326 binding domain) fused with an Fc fragment of a human  
327 IgG1 and expressed in *Drosophila* S2 cells (26–28); store  
328 at 4°C.
- 329 4. Secondary antibody (2 mg/mL): Alexa546-conjugated anti-  
330 human IgG (Invitrogen); store at 4°C.
- 331 5. Hoechst 33342 (Invitrogen): stock solution: 1 mM, working  
332 solution: 4 µM, final concentration: 2 µM, diluted in 1X PBS;  
333 store at –20°C.
- 334 6. Prolong Gold (Invitrogen).

Szekvolgyi et al.

**2.3. ChIP-on-Beads**

1. Nucleus isolation buffer: 5 mM Pipes, pH 8.0, 85 mM KCl, 0.5% NP-40, protease inhibitors (Sigma-Aldrich, cat no. P8340).
2. Sonication buffer: 1% SDS, 10 mM EDTA, 50 mM Tris-HCl, pH 8.0, protease inhibitors.
3. IP buffer: 0.01% SDS, 1.1% Triton X-100, 1.2 mM EDTA, 20 mM Tris-HCl pH 8.0, 167 mM NaCl, protease inhibitors.
4. Blocked protein A/G Sepharose (Upstate, cat. no. 16-157).
5. Antibodies (Upstate): anti-H4Kac, 2 µg/IP (cat. no. 06-866), anti-H3K4me2, 5 µg/IP (cat. no. 07-030).
6. Wash buffer (WB) A: 0.1% SDS, 1% Triton X-100, 2 mM EDTA, 20 mM Tris-HCl, pH 8.0, 150 mM NaCl, protease inhibitors.
7. WB B: 0.1% SDS, 1% Triton X-100, 2 mM EDTA, 20 mM Tris-HCl, pH 8.0, 500 mM NaCl, protease inhibitors.
8. WB C: 0.25 M LiCl, 1% NP-40, 1% Na-deoxycholate, 1 mM EDTA, 10 mM Tris-HCl, pH 8.0, protease inhibitors.
9. 1X TE: 10 mM Tris-HCl, pH 7.5, 1 mM EDTA.
10. QIAquick PCR Purification Kit (Qiagen).
11. Primers: forward 5'-*Fam*-GAGACCCTCCAAGTGCAC-3', reverse 5'-*Biotin*-CCAAAGCAGGGCTATAAGTTA GC-3'.
12. Streptavidin-coated microbeads (6 µm, Polyscience).

---

**3. Methods****3.1. ChIP-on-Beads**

1. Treat exponentially growing Jurkat cells with 40 µM etoposide (eto) for 3 h at 37°C to induce apoptosis.
2. Fix cells with 1% formaldehyde for 10 min at room temperature. Stop fixation by adding 2.5 M glycine to a final concentration of 0.67 M, for 5 min at room temperature. Wash cells twice in ice-cold PBS.
3. Resuspend cells in 1 mL of nucleus isolation buffer and incubate them for 10 min on ice. Vortex tubes in every 2–3 min.
4. Centrifuge isolated nuclei at 500 g for 3 min, at 4°C. Resuspend pellet in 500 µL sonication buffer.
5. Sonicate chromatin to an average fragment size of 500 bp using a Bioruptor (Diagenode); 0.5 min ON/0.5 min OFF pulses for 2 × 12 min usually produces the desired size distribution.

## Flow Cytometric and Laser Scanning Microscopic Approaches

- 385
- 386
- 387
- 388
- 389
- 390
- 391
- 392
- 393
- 394
- 395
- 396
- 397
- 398
- 399
- 400
- 401
- 402
- 403
- 404
- 405
- 406
- 407
- 408
- 409
- 410
- 411
- 412
- 413
- 414
- 415
- 416
- 417
- 418
- 419
- 420
- 421
- 422
- 423
- AQ4
- 424
- 425
- 426
- 427
- 428
- 429
- 430
- 431
- 432
6. Centrifuge sheared chromatin samples at maximum speed for 20 min. Keep supernatants (leave 50 µL on the bottom of the tubes). Freeze in liquid nitrogen and store samples at -80°C (or proceed immediately).
  7. Thaw samples on ice and centrifuge them at maximum speed for 10 min at 4°C. Transfer supernatants into clean tubes (do not disturb pellet on the bottom of the tubes).
  8. Dilute chromatin samples 1:10 in IP buffer as follows: 100 µL chromatin 900 µL IP buffer.
  9. Pre-clear samples by incubating them on a rotating wheel with 30 µL of blocked protein A/G Sepharose for 30 min at 4°C. Spin samples at 500g for 3 min at 4°C. Keep supernatants.
  10. Perform immunoselection for >12 h on a rotating wheel by adding the following antibodies to the samples: anti-H4Kac and anti-H3K4me2; as negative control, omit specific Ab but add a specific IgG protein from the same isotype to one of the pre-cleared samples.
  11. Preserve 10 µL from the ‘negative control’ as ‘input’ DNA and store it at -20°C. Collect immune complexes by adding 40 µL of blocked protein A/G Sepharose to each sample and incubate them for 45 min on a rotator. Spin samples at 500g for 3 min.
  12. Wash the pelleted immune complexes as follows: 2 × WB A, 2 × WB B, 2 × WB C, 1 × TE. Resuspend pellets in 500 µL TE. At this point thaw input DNA and dilute it to 500 µL; process it together with the IP samples.
  13. Reverse cross-links by incubating the samples at 98°C for 10 min. Put samples on ice.
  14. Digest residual RNAs with 200 µg/mL RNase A for 30 min at 37°C.
  15. Digest proteins by 0.5 mg/mL proteinase K for at least 2 h at 55°C.
  16. Purify DNA on PCR clean-up columns (Qiagen). Immuno-precipitated DNA samples (input, negative control, H4Kac/ H3K4me2, respectively) are ready to be tagged by *Fam/biotin* PCR.
  17. In the *Fam/biotin* PCR, use primers listed in **Section 2.3**. Perform PCRs under standard conditions and stop after 15–20 cycles, i.e., in the linear phase. Validate by QPCR (2). Purify the 5'-*Fam/biotin* labeled ChIP-PCR products on PCR clean-up columns.
  18. Carry out flow cytometry on a Becton-Dickinson FACScan flow cytometer as follows: 5 µL of the *Fam/biotin*-tagged ChIP-DNA was added to 10,000 streptavidin-coated, plain

433  
434  
435  
436  
437  
438  
439  
440  
441  
442  
443  
444  
445  
446  
447  
448  
449  
450  
451  
452  
453  
454  
455  
456  
457  
458  
459  
460  
461  
462  
463  
464  
465  
466  
467  
468  
469  
470  
471  
472  
473  
474  
475  
476  
477  
478  
479  
480

beads in 50 µL PBS. Incubate samples for 15 min at room temperature, wash in 1 mL PBS, and run at high speed. Set laser power to 15 mW and detect fluorescence signals through the 530/30 interference filter of the FL1 channel in logarithmic mode. Evaluate results using the BD<sup>®</sup> CELLQUEST 3.3 (Becton-Dickinson) software. TGM2 copy numbers are determined by reference to a standard curve obtained from a dilution series of known quantities of Fam/biotin-tagged PCR products (Fig. 7.1A). Express ChIP yields as percentage of input after subtracting background (no antibody (nAb) % of input).

### **3.2. Immunofluorescence and Laser Scanning Cytometry**

1. Grow HCT116 *DNMT1/3b* wt and *DNMT1/3b* knock-out cells on coverslips overnight.
2. Wash cells in 200 µL 1X PBS, 3 × 3 min.
3. Fix cells in a series of diluted methylalcohol (MetOH) (as shown below); wash cells with 200 µL of diluted MetOH once for 3 min, for each dilution. Start with the 10 × dilution. After washes, incubate cells in concentrated MetOH overnight at -20°C.

	<b>1X PBS (µL)</b>	<b>MetOH (µL)</b>
10 × MetOH	900	100
8 × MetOH	875	125
6 × MetOH	833	167
4 × MetOH	750	250
2 × MetOH	500	500

4. Rehydrate cells in a series of diluted 1X PBS as shown below; wash cells in 200 µL diluted MetOH for 3 min in each dilution. Start with the 10 × dilution. After the final rehydration step, wash with 200 µL 1X PBSs

	<b>MetOH (µL)</b>	<b>1X PBS (µL)</b>
10 × (1X PBS)	900	100
8 × (1X PBS)	875	125
6 × (1X PBS)	833	167
4 × (1X PBS)	750	250
2 × (1X PBS)	500	500

## Flow Cytometric and Laser Scanning Microscopic Approaches

- 481
- 482
- 483
- 484
- 485
- 486
- 487
- 488
- 489
- 490
- 491
- 492
- 493
- 494
- 495
- 496
- 497
- 498
- 499
5. In order to relax DNA, place samples into Petri dishes (without the cover) in PBS/1% BSA and irradiate them with UV light for 30 min.
  6. Immunolabel samples using the mCpG-specific MBD-Fc fusion protein or a commercially available Anti-5mC as primary antibody for 30 min at room temperature. Wash cells in 200  $\mu$ L of 1% BSA/PBS, 3  $\times$  for 3 min.
  7. Label samples with an Alexa546-conjugated anti-human IgG secondary antibody, for 30 min at room temperature. Wash cells in 200  $\mu$ L 1% BSA/PBS 3  $\times$  for 3 min.
  8. Stain DNA with 50  $\mu$ L Hoechst 33342 (2  $\mu$ M) and cover with Prolong Gold antifade.
  9. Scan slides (*see Note 1*).

---

**4. Notes**

- 500
- 501
- 502
- 503
- 504
- 505
- 506
- 507
- 508
- 509
- 510
- 511
- 512
- 513
- 514
- 515
- 516
- 517
- 518
- 519
- 520
- 521
- 522
- 523
- 524
- 525
- 526
- 527
- 528
1. MCpGs have been visualized using a Zeiss LSM 510 confocal laser-scanning microscope using excitation wavelengths of 543 and 351/364 nm. Fluorescence emission was detected through 560–615 and 385–470 nm band-pass filters. Images were taken in multitrack mode to prevent cross-talk between the channels. Pixel image (512  $\times$  512) stacks of 2–2.5  $\mu$ m thick optical sections were obtained with a 63  $\times$  Plan-Apochromat oil immersion objective (NA 1.4). The same samples were also analyzed using an iCys laser scanning cytometer (CompuCyte). The instrument used in our studies is equipped with a violet-blue diode, an argon-ion, and a HeNe laser (wavelengths 405, 488, and 633 nm, respectively). The violet and Ar-ion laser lines were used for excitation of Hoechst and Alexa 546 dyes. To identify single nuclei, contouring was based on Hoechst fluorescence detected in the blue channel (460–485 nm). Fluorescence of Alexa 546 (MCpGs) was detected in the orange channel (565–585 nm) based on the contour gained in the blue channel. In single nuclei identified by contouring on fluorescence of the nuclear stain, the integral fluorescence related to the MCpGs divided by the area of the contour was used to describe the methylation level. This corrects for differences in nuclear size. Data evaluation and hardware control were performed using the iCys 2.6 software for Windows XP. Using the 4  $\times$  objective to scan an indicated area on a slide, 400–1000 cells were scanned in about 10 min (21). LSC can screen relatively large number of cells on a slide. The cells are distinguished

529 based on their fluorescence properties like in flow cytometry.  
 530 However, as the position of each cell is fixed on the slide and  
 531 the instrument saves the positional information, any correlation  
 532 between the different parameters measured can be detected in a very sensitive manner. In addition, the cells can  
 533 be relocated and visually analyzed or re-scanned after re-staining  
 534 with conventional stains or fluorescent markers.  
 535

---

## Acknowledgments

541  
 542 The authors thank Drs. Rolf Ohlsson and Anita Göndör (Uppsala,  
 543 Sweden) for the DNMT-KO and control HCT116 cells and Dr.  
 544 Michael Rehli (Regensburg, Germany) for the stably transfected  
 545 *Drosophila Schneider 2*(S2) cell line producing the MBD-Fc fusion  
 546 protein. This publication was sponsored by OTKA fundings  
 547 TO48742, OTKA 72762, and the research grant of the Ministry  
 548 of Public Health ETT 067/2006.  
 549

## References

- 550
- 551
- 552
- AQ5
- Pataki, J., Szabo, M., Lantos, E., Szekvolgyi, L., Molnar, M., Hegedus, E., Bacso, Z., Kappelmayer, J., Lustyik, G. and Szabo, G. (2005) Biological microbeads for flow-cytometric immunoassays, enzyme titrations, and quantitative PCR. *Cytometry* **68**, 45–52.
  - Szekvolgyi, L., Balint, B. L., Imre, L., Goda, K., Szabo, M., Nagy, L. and Szabo, G. (2006) Chip-on-beads: flow-cytometric evaluation of chromatin immunoprecipitation. *Cytometry* **69**, 1086–1091.
  - Balint, B. L., Szanto, A., Madi, A., Bauer, U. M., Gabor, P., Benko, S., Puskas, L. G., Davies, P. J. and Nagy, L. (2005) Arginine methylation provides epigenetic transcription memory for retinoid-induced differentiation in myeloid cells. *Mol. Cell Biol.* **25**, 5648–5663.
  - Downs, J. A. and Jackson, S. P. (2003) Cancer: protective packaging for DNA. *Nature* **424**, 732–734.
  - Hake, S. B., Xiao, A. and Allis, C. D. (2004) Linking the epigenetic ‘language’ of covalent histone modifications to cancer. *Br. J. Cancer* **90**, 761–769.
  - Seligson, D. B., Horvath, S., Shi, T., Yu, H., Tze, S., Grunstein, M. and Kurdistani, S. K. (2005) Global histone modification patterns predict risk of prostate cancer recurrence. *Nature* **435**, 1262–1266.
  - Lafon-Hughes, L., Di Tomaso, M. V., Mendez-Acuna, L. and Martinez-Lopez, W. (2008) Chromatin-remodelling mechanisms in cancer. *Mutat. Res.* **658**, 191–214.
  - Fanelli, M., Caprodossi, S., Ricci-Vitiani, L., Porcellini, A., Tomassoni-Ardori, F., Amatori, S., Andreoni, F., Magnani, M., De Maria, R., Santoni, A., Minucci, S. and Pelicci, P. G. (2008) Loss of pericentromeric DNA methylation pattern in human glioblastoma is associated with altered DNA methyltransferases expression and involves the stem cell compartment. *Oncogene* **27**, 358–365.
  - Piyathilake, C. J., Frost, A. R., Bell, W. C., Oelschlager, D., Weiss, H., Johanning, G. L., Niveleau, A., Heimburger, D. C. and Grizzle, W. E. (2001) Altered global methylation of DNA: an epigenetic difference in susceptibility for lung cancer is associated with its progression. *Hum. Pathol.* **32**, 856–862.
  - Estecio, M. R., Gharibyan, V., Shen, L., Ibrahim, A. E., Doshi, K., He, R., Jelinek, J., Yang, A. S., Yan, P. S., Huang, T. H., Tajara, E. H. and Issa, J. P. (2007) LINE-1

## Flow Cytometric and Laser Scanning Microscopic Approaches

- hypomethylation in cancer is highly variable and inversely correlated with microsatellite instability. *PLoS ONE* **2**, e399.
11. Ogino, S., Kawasaki, T., Noshio, K., Ohnishi, M., Suemoto, Y., Kirkner, G. J. and Fuchs, C. S. (2008) LINE-1 hypomethylation is inversely associated with microsatellite instability and CpG island methylator phenotype in colorectal cancer. *Int. J. Cancer* **122**, 2767–2773.
  12. Shimabukuro, M., Sasaki, T., Imamura, A., Tsujita, T., Fuke, C., Umekage, T., Tochigi, M., Hiramatsu, K., Miyazaki, T., Oda, T., Sugimoto, J., Jinno, Y. and Okazaki, Y. (2007) Global hypomethylation of peripheral leukocyte DNA in male patients with schizophrenia: a potential link between epigenetics and schizophrenia. *J. Psychiatr. Res.* **41**, 1042–1046.
  13. Matarazzo, M. R., Boyle, S., D'Esposito, M. and Bickmore, W. A. (2007) Chromosome territory reorganization in a human disease with altered DNA methylation. *Proc. Natl. Acad. Sci. U.S.A.* **104**, 16546–16551.
  14. Miranda, T. B. and Jones, P. A. (2007) DNA methylation: the nuts and bolts of repression. *J. Cell Physiol.* **213**, 384–390.
  15. Rhee, I., Bachman, K. E., Park, B. H., Jair, K. W., Yen, R. W., Schuebel, K. E., Cui, H., Feinberg, A. P., Lengauer, C., Kinzler, K. W., Baylin, S. B. and Vogelstein, B. (2002) DNMT1 and DNMT3b cooperate to silence genes in human cancer cells. *Nature* **416**, 552–556.
  16. Sun, L., Zhao, H., Xu, Z., Liu, Q., Liang, Y., Wang, L., Cai, X., Zhang, L., Hu, L., Wang, G. and Zha, X. (2007) Phosphatidyl-inositol 3-kinase/protein kinase B pathway stabilizes DNA methyltransferase I protein and maintains DNA methylation. *Cell Signal* **19**, 2255–2263.
  17. Kuo, M. H. and Allis, C. D. (1999) In vivo cross-linking and immunoprecipitation for studying dynamic protein:DNA associations in a chromatin environment. *Methods* **19**, 425–433.
  18. Taylor, J. D., Briley, D., Nguyen, Q., Long, K., Iannone, M. A., Li, M. S., Ye, F., Afshari, A., Lai, E., Wagner, M., Chen, J. and Weiner, M. P. (2001) Flow cytometric platform for high-throughput single nucleotide polymorphism analysis. *Biotechniques* **30**, 661–666, 668–669.
  19. Spiro, A. and Lowe, M. (2002) Quantitation of DNA sequences in environmental PCR products by a multiplexed, bead-based method. *Appl. Environ. Microbiol.* **68**, 1010–1013.
  20. Bacso, Z., Everson, R. B. and Eliason, J. F. (2000) The DNA of annexin V-binding apoptotic cells is highly fragmented. *Cancer Res.* **60**, 4623–4628.
  21. Bacso, Z. and Eliason, J. F. (2001) Measurement of DNA damage associated with apoptosis by laser scanning cytometry. *Cytometry* **45**, 180–186.
  22. Khobta, A., Carlo-Stella, C. and Capranico, G. (2004) Specific histone patterns and acetylase/deacetylase activity at the breakpoint-cluster region of the human MLL gene. *Cancer Res.* **64**, 2656–2662.
  23. Beck, S. and Rakyan, V. K. (2008) The methylome: approaches for global DNA methylation profiling. *Trends Genet.* **24**, 231–237.
  24. Habib, M., Fares, F., Bourgeois, C. A., Bella, C., Bernardino, J., Hernandez-Blazquez, F., de Capoa, A. and Niveleau, A. (1999) DNA global hypomethylation in EBV-transformed interphase nuclei. *Exp. Cell Res.* **249**, 46–53.
  25. Adouard, V., Dante, R., Niveleau, A., Delain, E., Revet, B. and Ehrlich, M. (1985) The accessibility of 5-methylcytosine to specific antibodies in double-stranded DNA of *Xanthomonas* phage XP12. *Eur. J. Biochem.* **152**, 115–121.
  26. Gebhard, C., Schwarzfischer, L., Pham, T. H., Andreesen, R., Mackensen, A. and Rehli, M. (2006) Rapid and sensitive detection of CpG-methylation using methyl-binding (MB)-PCR. *Nucleic Acids Res.* **34**, e82.
  27. Gebhard, C., Schwarzfischer, L., Pham, T. H., Schilling, E., Klug, M., Andreesen, R. and Rehli, M. (2006) Genome-wide profiling of CpG methylation identifies novel targets of aberrant hypermethylation in myeloid leukemia. *Cancer Res.* **66**, 6118–6128.
  28. Schilling, E. and Rehli, M. (2007) Global, comparative analysis of tissue-specific promoter CpG methylation. *Genomics* **90**, 314–323.